PASJ: Publ. Astron. Soc. Japan **44**, 421–433 (1992)

Millimeter-Wave Continuum around NGC 7538-IRS1, IRS2, and IRS3

Kenji AKABANE and Shozo TSUNEKAWA
Department of Physics, Faculty of Science, Toyama University, 3190, Gofuku, Toyama 930

Makoto INOUE, Ryohei KAWABE, Nagayoshi OHASHI, Osamu KAMEYA, and Masato ISHIGURO
Nobeyama Radio Observatory, Minamimaki-mura Minamisaku-gun, Nagano 384-13*
and
Yoshiaki SOFUE
Institute of Astronomy, The University of Tokyo, Mitaka, Tokyo 181

(Received 1991 October 9; accepted 1992 February 24)

Abstract

Millimeter-wave continuum sources in the NGC 7538 region were observed with the NRO 45-m telescope and Nobeyama Millimeter Array (NMA). NRO 45-m telescope observations showed that the compact region which includes IRS1, 2, and 3 has a strong millimeter-wave intensity excess. This region was also studied with NMA at 49 and 98 GHz, and the obtained millimeter-wave spectrum was analyzed. It has been proposed from this analysis that new compact quasi-spherical and homogeneous H II sources may exist in the IRS1 region, rather than the VLA ultra-compact H II regions. It is suggested that the new sources have a small linear size, of the order of 10^{15} cm, and a high electron density of $\sim 10^7$ cm^{-3}; they are still optically thick, even in the 100 GHz range. This gives an H II evolution time as short as about 100 yr. These small, but intense, H II emission sources in IRS1 may well be identified by cocoon stars. To investigate the evolution of the H II regions in the cocoon, an intensity monitoring observation, as well as a source expansion check, of NGC 7538-IRS1 at around 49 GHz in about 10 yr has been proposed. The total flux density of the extended dust emission around IRS1 was estimated to be about 0.6 Jy at 90 GHz, giving a somewhat steeper intensity spectrum than ν^3.

Key words: Cocoon stars — Compact H II regions — Evolution of H II region — Millimeter-wave dust emission — NGC 7538-IRS1

1. Introduction

Radio emission of the entire region of NGC 7538 has been observed mostly by interferometers down to the cm-wave region (Habing et al. 1972; Israel et al. 1973; Martin 1973; Wink et al. 1975; Israel 1977). This region was resolved into an extended main area and nearby compact sources. One of the compact sources was associated with the OH maser source (Martin 1973). The source was also observed with a 15-GHz 0.″7 beam, giving a typical thermal spectrum for the source, denoted as NGC 7538(B) (Harris and Scott 1976). A cluster of infrared sources (NGC 7538-IRS1, 2, and 3) was found by Wynn-Williams et al. (1974) in this OH maser region. More extensive, physical studies, as well as the wide region of NGC 7538, were made by Werner et al. (1979).

VLA observations at 24 GHz revealed a compact H II region associated with IRS1; a turnover frequency at around 20 GHz was suggested (Henkel et al. 1984). Turner and Matthews (1984) as well as Campbell (1984) found an ultra-compact fine structure of the IRS1 H II region with a resolution of 0.″3–0.″1 at 5 and 15 GHz, giving an optically thick spectrum of the region. On the other hand, Scoville et al. (1986) made a 110 GHz continuum observation of this region, and obtained a rather intense mm-wave flux density with IRS1, as 2.55 Jy. Although they investigated thermal emission from optically thin dust grains for this intense mm-wave emission, they associated their 110-GHz flux density directly to the Campbell's 15-GHz result (1984), 0.418 Jy, to find the spectral index of the source. They then preferred a stellar wind H II region model (Panagia and Felli 1975; Wright and Barlow 1975), rather than dust grain emission, and obtained a spectrum which increases roughly as $\nu^{0.6}$, ν being the frequency.

Single-dish observations of NGC 7538 region were made by Schraml and Mezger (1969) at a wavelength of 1.95 cm, and by Gordon et al. (1986) at 84.2 GHz.

* Nobeyama Radio Observatory (NRO) is a branch of the National Astronomical Observatory, an inter-university research institute operated by the Ministry of Education, Science and Culture.

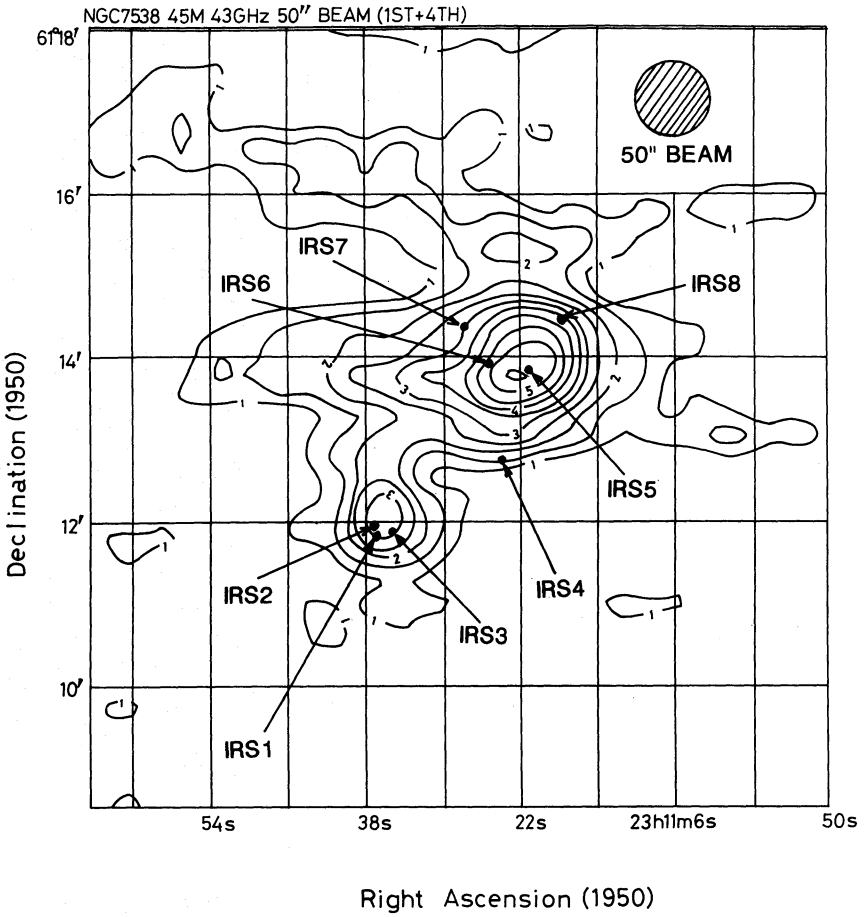

Fig. 1. 43-GHz intensity map of the NGC 7538 region. The re-convolved resolution is 50″, and the contour unit is 115 mK in T_B (brightness temperature). The peak brightness temperatures (T_{BP}) are 0.64 and 0.4 K for the diffuse main and compact areas, respectively. The positions of the IRS1, 2, and 3 [from Hackwell et al. (1982)] and those of the IRS4–8 [from Wynn-Williams et al. (1974)]; they are given by the arrows in each area. The observed results are listed in table 1.

The re-convolved map at 2′ resolution of the 84.2-GHz result was compared by Gordon et al. (1986) with the 1.95-cm same resolution map of the region, as shown in the bottom of their figure 3j. Although the resolution is as low as 2′, we can still see in the figure some 84.2 GHz excess intensity concentration around ($\alpha = 23^h11^m36^s$, $\delta = 61°12'$), suggesting that there exists a mm-wave excess, which becomes visible only in the optically thin or diffuse area of the region. The position of the 84.2 GHz excess emission strongly suggests that it is associated with the NGC 7538-IRS1 complex.

An aim of the present work is to find the concentration of mm-wave excess emission at 90 GHz relative to that at 43 GHz in the NGC 7538 region with a high resolution of $\sim 50''$. Another point of the present observations with the NRO 45-m telescope is to obtain the total flux densities of IRS1, 2, and 3 at 43 GHz and 90 GHz, and to make critical check of the procedure by which Scoville et al. (1986) found that the radio spectrum of IRS1 increased continuously with frequency from 15GHz (Campbell 1984) to 110 GHz.

A localized 90-GHz excess emission was found in the region with the 45-m telescope survey; the Nobeyama Millimeter Array (NMA) could then be available to find mm-wave fine structure of the source. Preliminary 49-GHz and 98-GHz NMA observations of this region, with its A, B, C, and D configurations for synthesized beams of 5″ and 2″, respectively, have been successively carried out in the present study.

2. Observations with the NRO 45-m Telescope

New 43-GHz and 90-GHz continuum observations of the NGC 7538 region were made in 1989 February with the 45-m telescope at Nobeyama Radio Observatory (NRO). Two-frequency (45 and 90 GHz) signals which

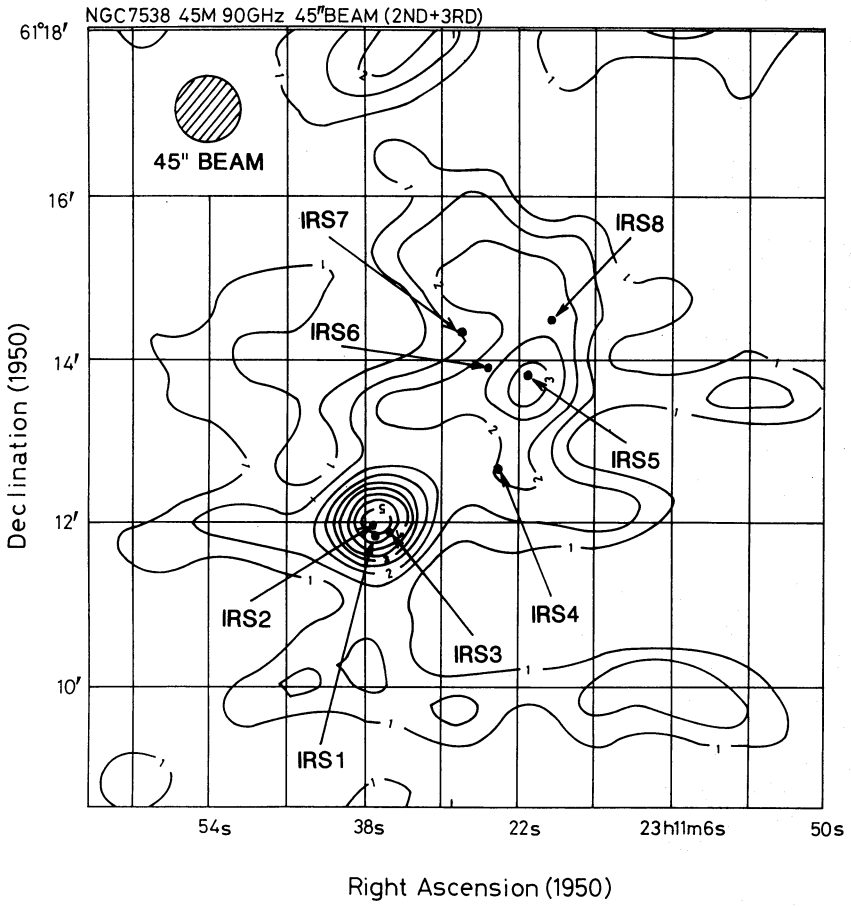

Fig. 2. 90-GHz intensity map of the NGC 7538 region. The re-convolved resolution is 45″, and the contour unit is 40 mK in T_B (brightness temperature). The peak brightness temperatures (T_{BP}) are 0.13 and 0.21 K for the diffuse main and the compact areas, respectively. The positions of the infrared sources are given as in figure 1. The observed results are listed in table 1.

were divided by a polarization splitter in the transmission guide of the 45-m telescope were observed simultaneously. The 43-GHz receiver was sensitive in two 800 MHz bandwidths at both center frequencies of 43 ± 1.5 GHz (DSB) and a 43-GHz SIS receiver, which was developed at NRO. It had a system noise temperature of 230 K (DSB) at the zenith. The 90-GHz receiver was sensitive in two 500 MHz bandwidths at 90.0 ± 1.4 GHz (DSB). A He-cooled Schottky-barrier diode mixer at 90 GHz (provided by the Millitech Co.) was employed, giving a system noise temperature of about 380 K (DSB) at the zenith. The original beamwidths of the telescope were measured to be typically 24″ × 24″ (FWHM) and 45″×45″ (FWHM) at 90 and 43 GHz, respectively, by observing the compact H II region NGC 7027 at less windy times. The peaks of nearby localized sidelobes for both frequencies were estimated to be generally less than 5% of each main beam. A beam-switching system, in which the reference beam is separated by 8° for both frequencies in the azimuth direction, was employed.

Intensity calibrations were made for both frequencies by observing NGC 7027, in which the flux densities at 43 and 90 GHz were each taken to be 6.0 Jy, as extrapolated from the 15-GHz observation by Harris and Scott (1976). Ori A (Trapezium stars 46-GHz peak of 5.5 K in T_B; Akabane et al. 1985) was partly used for the intensity calibration. The pointing errors were also estimated from these objects to be less than ±10″ for both frequency observations.

The mapping area for both frequencies was selected to be as large as 10′ × 10′, and centered at R.A. = $23^h11^m26^s.5$ and Decl. = 61°13′09″ (1950.0). Right-ascension scans for each declination step of 15″ were made continuously. Smoothed maps were obtained by the press method (Sofue and Reich 1979), and original maps at 43 and 90 GHz were re-convolved by a Gaussian

beam to have resolutions of 50″ and 45″, respectively, in order to eliminate any wind effects or receiver instabilities.

The intensity maps for both frequencies are given in figures 1 and 2. Both maps were obtained simultaneously with the use of the polarization beam splitter; the directions of receiving polarization which rotate with time were then determined. A random polarization of the source was therefore assumed throughout the construction of the maps. The observational parameters obtained from figures 1 and 2 are listed in table 1, along with the 5-GHz interferometer results obtained by previous workers for a comparison of the flux densities in the corresponding area.

It is remarkable that the ratio of the flux densities which were observed for the compact and diffuse main areas in the region, $S_{\nu c}/S_{\nu d}$ in table 1, at 90 GHz is larger than 1/5, while those at other frequencies are fairly constant, and less than 1/10. This suggests that the compact and diffuse main sources of NGC 7538 are both optically thin, except for the 90 GHz brightness of the compact source. A sudden increase of 90-GHz flux density of the compact region relative to that of 43 GHz is also clear in figures 1 and 2. The ratio of $S(90)_c/S(43)_c$, (3.0±1.0 Jy)/(1.3±0.4 Jy)∼2.3, in table 1 is reasonably reliable in so far as the observed ratio of $S(90)_d/S(43)_d$, (14±5 Jy)/(17±5 Jy)∼0.85, can be assumed to be roughly equal to (90 GHz/43 GHz)$^{-0.1}$(=0.93) for the optically thin model of the source (Mezger and Henderson 1967). The 43-GHz and 90-GHz flux densities listed in table 1 are plotted in figure 3 with published results at low frequencies for a comparison. Marks K and J in figure 3, which were obtained by the 45-m telescope for the diffuse main area of NGC 7538, are nearly on an optically thin flat thermal spectrum [(A1) in figure 3] which was deduced from the low-frequency results. This means that in this region there are no conspicuous sources which are optically thick in the mm-wave region; the region is optically thin everywhere. On the other hand, results H and F, (A2) in figure 3, for the compact region containing IRS1, 2, and 3 sources of NGC 7538 as figures 1 and 2 show a steep mm-wave excess; this means that some of the sources of IRS1, 2, and 3 must be optically thick, even in the mm-wave region at 3 mm.

A preliminary report on these 45-m mm-wave observations has been made by Akabane et al. (1991).

3. Observations with the Nobeyama Millimeter Array (NMA)

VLA observations by Campbell (1984), as well as by Turner and Matthews (1984) showed an ultra-compact H II region, NGC 7538-IRS1, with a size somewhat less than $(1'')^2$ at both 5 and 15 GHz. An OVRO synthesis observation of this source was made at 2.7 mm by Scoville et al. (1986) with a resolution of 7″; they assumed that there is only one H II region associated with IRS1 which emits 5-GHz, 15-GHz, and 110-GHz (2.7 mm) continuum, as observed. Accordingly, they postulated an optically thick spectrum that increases up to 110 GHz as a mass-loss stellar wind model of the source (Panagia and Felli 1975; Wright and Barlow 1975).

In the present study, a clear 90-GHz excess emission in the compact area of NGC 7538-IRS1, 2, and 3 was found with the 45-m telescope observations, as shown in figure 2, table 1, and in figure 3 (H–F). Then, the observations by the Nobeyama Millimeter Array (NMA) at 49 and 98 GHz for this compact area were immediately proposed in order to investigate the high-resolution millimeter-wave structure of the region.

3.1. Observations

NMA observations were made with synthesized nearly circular beams of 6.″0 × 5.″5 at 49 GHz and 2.″9 × 2.″3 at 98 GHz in 1988 December and in the beginning of 1990, respectively. In addition to 49- and 98-GHz continuum emission, CS(1–0) and CS(2–1) molecular lines have also been observed; the results will be presented in separate papers. We used SIS receivers (Kawabe et al. 1990) for both the 49- and 98-GHz observations. Source BL Lac, ($\alpha = 22^h00^m39^s.363$, $\delta = 42°02'8''.57$, 1950.0) was used for the phase calibration at both 49 and 98 GHz; the absolute position accuracy was estimated to be about ±0″.5. An intensity calibration was made by also referring to source BL Lac, with flux densities of 3.5 Jy and 2.1 Jy at 49 and 98 GHz, respectively, during each observation period. The flux densities of the calibration sources were measured by observing the planets; their uncertainties were ±20%. Reduction was made with the use of "AIPS"; the two-frequency NMA cleaned continuum results are shown in figures 4 and 5, where the compact (IRS1, 2, and 3) area in figures 1 and 2 was selected as the field of each NMA observation.

It is clear in figure 4 that although the compact area (see table 1) is resolved into IRS1 and IRS2 components with a 49-GHz resolution of 6.″0 × 5.″5, IRS3 could not be detected, though 1σ of noise fluctuation of the sky was estimated to be 11 mJy/beam. The IRS1 and IRS2 region has so far been resolved into two components by only cm-wave interferometers (Martin 1973; Israel 1977; Campbell and Persson 1988). Figure 4 is the first radio map of IRS1 which shows the separate component of IRS2 in the mm-wave region. Although the region of IRS1 is not resolved, that of IRS2 is extended.

The contour map obtained at 98 HGz is shown in figure 5. The region is again resolved with a 98-GHz synthesized beam of 2.″9 × 2.″3 into two components comprising a compact core of IRS1 and an extended component of IRS2. The compact core component (IRS1) is hardly

Table 1. List of the observational data collected by the 45-m telescope. The 45-m results of the NGC 7538 diffuse main and compact regions are listed, where the beamwidths are re-convolved Gaussian beamwidths by computer, T_{BP} is the brightness temperature at the contour peak of each area, the size ($\Delta\alpha \times \Delta\delta$) is the observed width (FWHM) of each area in α and δ directions, and $S_{\nu d}$ and $S_{\nu c}$ are the integrated flux densities of the diffuse and compact areas at frequency ν, respectively. 2″ and 7″ beam data at 5 GHz are reproduced from the studies by Martin (1973) and Israel (1977), respectively. $S_{\nu c}$ was named "G total" by Israel (1977).

Source name	Frequency Beamwidth	43 GHz $(50'')^2$	90 GHz $(45'')^2$	5 GHz $(2'')^2$	5 GHz $(7'')^2$
	Peak position (α, $\delta \pm 5''$, 1950.0)	...	α=23^{h}11^{m}22^s δ= 61°13′45″	...	...
Diffuse main (IRS4+IRS5+IRS6+IRS7+IRS8)	T_{BP} (K) Size ($\Delta\alpha \times \Delta\delta$) (obs)	0.64±0.2 ∼(115″×135″)	0.13±0.04 ∼(115″×135″)	...	...
	$S_{\nu d}$(Jy)	17±5	14±5	...	19.1
	Peak Position (α, $\delta \pm 5''$, 1950.0)	...	α=23^{h}11^{m}37^s δ= 61°12′00″	...	...
Compact (IRS1+IRS2+IRS3)	T_{BP} (K) Size ($\Delta\alpha \times \Delta\delta$) (obs)	0.40±0.1 (50″×50″)	0.21±0.07 (45″×45″)	... ...	... ...
	$S_{\nu c}$ (Jy)	1.3±0.4	3.0±1.0	1.5	1.4

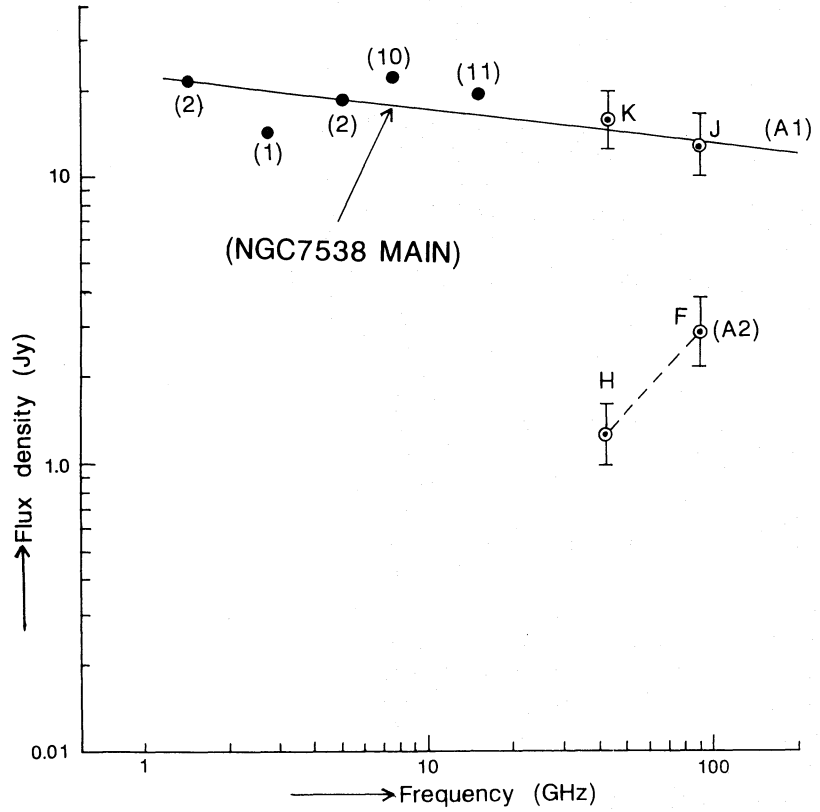

Fig. 3. Continuum spectra of the sources in NGC 7538 region. (A1) is for the diffuse main area of the region, as noted in table 1, where the present 45-m results (dotted circles K and J) are combined with data by other workers as (1): Martin (1973), (2): Israel (1977), (10): Lada and Chaisson (1973), and (11): Schraml and Mezger (1969). (A2), dotted circles H and F, is for the compact area of NGC 7538, as shown in table 1.

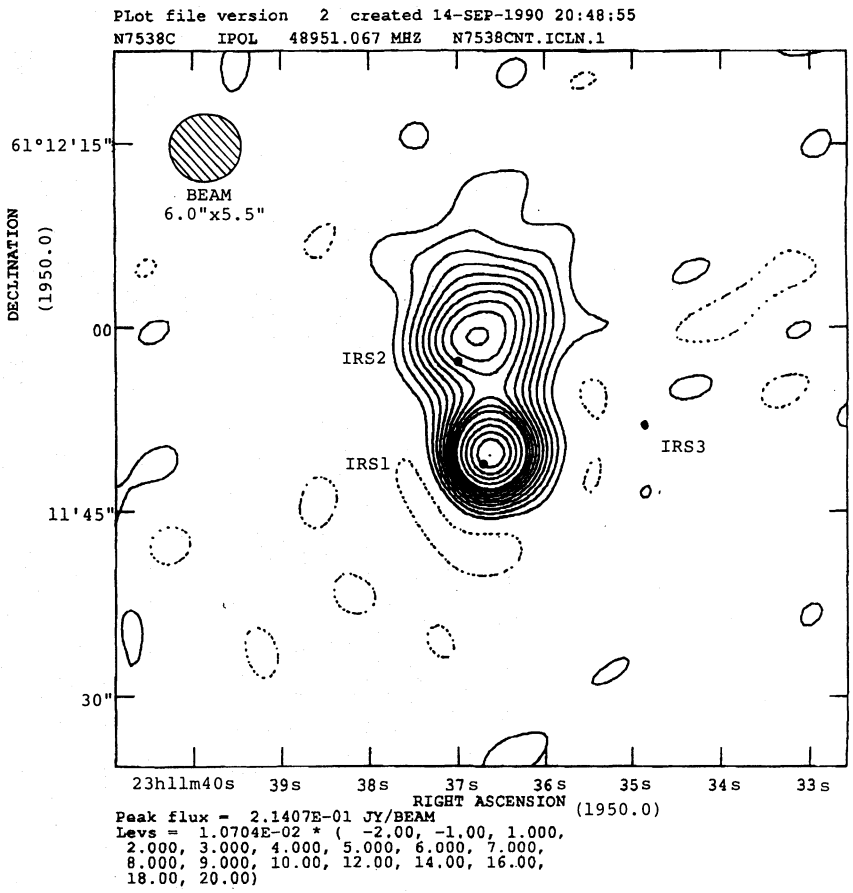

Fig. 4. 49-GHz contour map of the IRS1, 2, and 3 region by the NMA with a synthesized beamwidth of 6.″0 × 5.″5. The observed results are listed in table 2. The dots indicate the positions of IRS1, 2, and 3 (Wynn-Williams et al. 1974).

resolved, but the extended component (IRS2) shows a complicated structure, as can be seen in the cm-wave interferometer results (Martin 1973; Campbell and Persson 1988). However, a slightly more complex structure can be seen in the mm-wave map of the region than that seen in the cm-wave region. This may give a more intrinsic distribution of the emission measure in the region, due to its small optical thickness. The OVRO IRS1 110-GHz map of this region (Scoville et al. 1986), with a beam of 7″, may include some confusion from the IRS2 component. The map in figure 5 is the first 100-GHz map of IRS1 accompanied by a widely extended component of IRS2.

The IRS3 component was not detected by the 98-GHz NMA with a sky noise fluctuation of 1σ of 9 mJy/beam.

The physical parameters which were derived from figures 4 and 5 are summarized in table 2.

3.2. IRS1

The IRS1 region was observed as the component "G1" by Israel (1977). The flux densities of IRS1 at 49 and at 98 GHz, which were obtained from synthesis maps (figures 4 and 5) are plotted in figure 6 (open circles) along with other data from (7) (Henkel et al. 1984) and (8) (Woody et al. 1989) (filled circles). A smoothed curve, which is given by a dashed line (O) in figure 6, was fitted so as to trace four of these data. Data (5) (Scoville et al. 1986) was not used, because it may include some of the IRS2 H II emission as well as some of Werner's extended dust emission around the IRS1 (Werner et al. 1979) due to the large beamwidth of 7″ in the observation. The dashed smoothed curve (O) seems to comprise two independent thermal spectra of spherical sources with different turnover frequencies. We then divided the spectrum (O) into two thermal spectra [(A) and (B)], as shown in figure 6, in the following way. A computed spectrum (A) with a turnover frequency at 10 to 15 GHz was used to fit the thermal emission from the centrally condensed urtra-compact VLA H II region, by Campbell (1984), and by Turner and Matthews (1984). This procedure was also discussed, and suggested by Harris and Scott (1976), Henkel et al. (1984), as well as by Turner

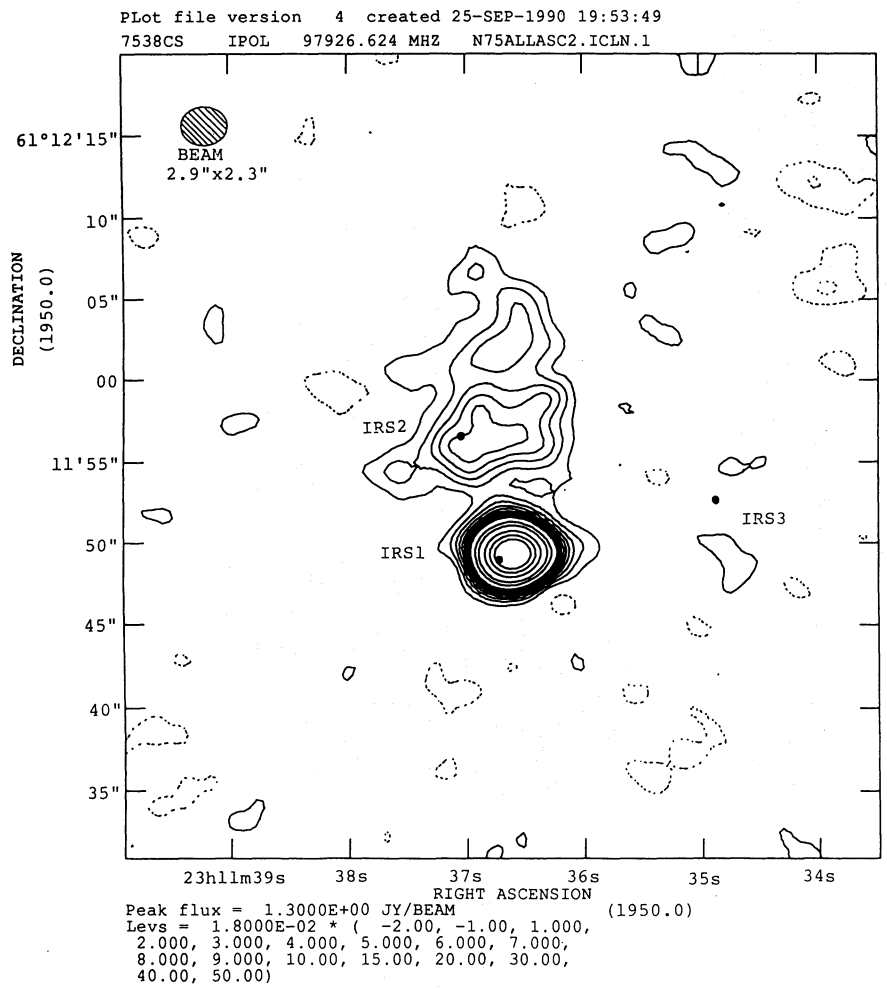

Fig. 5. 98-GHz contour map of the IRS1, 2, and 3 region by the NMA with a synthesized beamwidth of $2''.9 \times 2''.3$. The observed results are listed in table 2. The dots are for the positions of IRS1, 2, and 3 (Wynn-Williams et al. 1974).

and Matthews (1984). When we subtract spectrum (A) from the observed spectrum (O) in figure 6, we obtain filled triangles from data (7) (Henkel et al. 1984) and (8) (Woody et al. 1989), and open triangles from the present NMA results. The residuals, 4 triangles in figure 6, seem to make a single thermal spectrum of a spherical homogeneous source, as a computed spectrum (B) in figure 6, in good coincidence. We have assumed here that the source for (B) is very compact and that an overlap effect with that for (A), if it exists, can be ignored for simplicity. Thermal spectrum (B) has a turnover frequency at 100 to 200 GHz, suggesting the existence of a new compact H II source, rather than a dust-emission source, in addition to Campbell's (1984) ultra-compact H II source. A new source with spectrum (B) would be intense, but its size would be much smaller than the Campbell's (1984) H II region, and would become visible only at around 20 GHz or higher. We propose here a new H II source with spectrum (B), instead of spectrum (O) which was connected directly to the 15-GHz flux density of the ultra compact H II region (Campbell 1984), to obtain a single source of an optically thick thermal spectrum up to 110 GHz, as was shown by Scoville et al. (1986) using their stellar wind model. If this is the case, the effective source size of Campbell's (1984) H II region at 15 GHz must become smaller at higher frequencies. The actually estimated source size at 98 GHz [$\sim(1''.2)^2$ as in table 2], however, seems to be somewhat larger than $\sim 1'' \times 0''.5$ of the 15-GHz source size (Campbell 1984). Data (9), C in figure 6, is from a 1-mm observation of the IRS1 region by Werner et al. (1979). Their intensity spectrum, derived from 30, 50, and 100 μm observations with large apertures, gives a lower limit of the extension of dust emission of IRS1 as being about $15'' \times 15''$. In the mm-wave region this widely extended ($> 15'' \times 15''$) dust emission may be assumed to have a ν^3 (ν being the frequency)

Table 2. Results from the NGC 7538 compact area by the NMA. NRO millimeter array observational results at 49 and 98 GHz are listed. S_ν(total), S_ν(A), and S_ν(B) are for spectra (O), (A), and (B) in figure 6, respectively. The intrinsic source sizes [(~FWHM) θ_i] were simply derived as $\theta_i^2 = \theta_{obs}^2 - \theta_{beam}^2$. The peak position of IRS2 is subject to a large uncertainty because of the extended area of this source.

Source name	Frequency Beamwidth (″)×(″)	49 GHz 6.0×5.5	98 GHz 2.85×2.26
IRS1	Peak position (α, δ±1″;1950.0)	α=23^{h}11^{m}36^s.6 δ=61°11′49″.5	α=23^{h}11^{m}36^s.6 δ=61°11′49″.2
	S_ν (total) (Jy)	0.9±0.2	1.6±0.3
	S_ν (A) (Jy)	0.5	0.5
	S_ν (B) (Jy)	0.4	1.1
	θ_{obs}^2 ($\Delta\alpha \times \Delta\delta$) (″)×(″)	5.7×6.2	3.1×2.6
	θ_i^2 (″)^2	(~1.5±0.6)^2	(1.2±0.6)^2
IRS2	Peak position (α, δ±1″;1950.0)	α=23^{h}11^{m}36^s.8 δ=61°11′59″.2	α=23^{h}11^{m}36^s.9 δ=61°11′57″
	S_ν (Jy)	1.1±0.2	1.0±0.2
	θ_{obs}^2 ($\Delta\alpha \times \Delta\delta$) (″)×(″)	~9.5×9.5	6.4×7.9
	θ_i^2 (″)^2	(~7.6)^2	(~6.7)^2
IRS3	S_ν (Jy)	<0.02	<0.02

spectrum, as C–E in figure 6. This gives ~ 10 Jy at the 1.4-mm region of Woody et al. (1989); the beamwidth of the OVRO interferometer at 1.4 mm, however, was as sharp as (3.″3)^2. The confusion from this extended dust emission into data (8) was thus estimated to be much less than 0.5 Jy. In the same way, the flux-density confusion regarding each triangle (open and filled in figure 6) from this extended dust emission can be roughly ignored, due to their interferometric steep concentration of the source. Due to this confusion, therefore, no big change may be expected regarding spectrum (B) in figure 6.

Dotted circle D in figure 6 represents the 90-GHz flux density from the extended dust around IRS1, by Werner et al. (1979). This was estimated in such a way that flux density D must be a remainder of the 90-GHz total flux density of the compact given in table 1, when $S(90)_c$ in table 1 is subtracted by the interferometric total flux densities of IRS1, IRS2, and IRS3: that is to say, 3.0 Jy [= $S(90)_c$: total of the compact]−{1.4 Jy [=total of IRS1: (A)+(B) in figure 6]+1.0 Jy [=total of IRS2 and IRS3: (B)+(C) in figure 7]}=0.6 Jy (=remainder). Probable 90-GHz flux densities of IRS2 and IRS3 used here could be estimated from figure 7 separately. The 90-GHz remainder of 0.6 Jy derived here can be attributed to an extended diffuse source, the emission of which could be detected only by a filled aperture dish observation, such as the present work, and is hardly included in interferometries as the spectrum (O) in figure 6. Confusion concerning the extended dust emission source observed by Werner et al. (1979) into the observed interferometric contours were estimated to be less than 0.02 Jy and 0.04 Jy at 49 GHz and 98 GHz, respectively, assuming a ν^3 spectrum as C–E in figure 6 for this extended dust emission. We can connect C and D in figure 6 as the thermal spectrum of Werner's extended dust emission, though flux density D would be subject to a large observational error, as shown in table 1. Spectrum D–C seems to be slightly steeper than ν^3, as can be seen in figure 6. The 90-GHz flux densities for each source component are also given in table 3.

The intrinsic source size (θ_i^2) of the IRS1 at the mm-wave region, which is simply estimated to be $\theta_i^2 = \theta_{obs}^2 - \theta_{beam}^2$ [(1.2)^2−(1.5)^2] in table 2, seems to be fairly larger than ~ 1″ × 0″.5 of Campbell's ultra-compact H II region in IRS1 at 5 and 15 GHz (Campbell 1984), possibly having spectrum (A) in figure 6. This means that the newly derived mm-wave component (B) in figure 6 must have extended or scattered H II emission sources associated with Campbell's (1984) H II source in IRS1. The observational peak position of the (A)+(B) components at 98 GHz (as listed in table 2) is in good coincidence with Campbell's (1984) H II source with spectrum (A) in figure 6, within a ±1″ error. The physical structure of component (B) is discussed in the next section. In table 3 the flux densities of the source components of IRS1 at each frequency are summarized.

Pratap et al. (1989) also discussed the two-component structure of the IRS1 H II source, requiring an optically thin area in the mm-wave region.

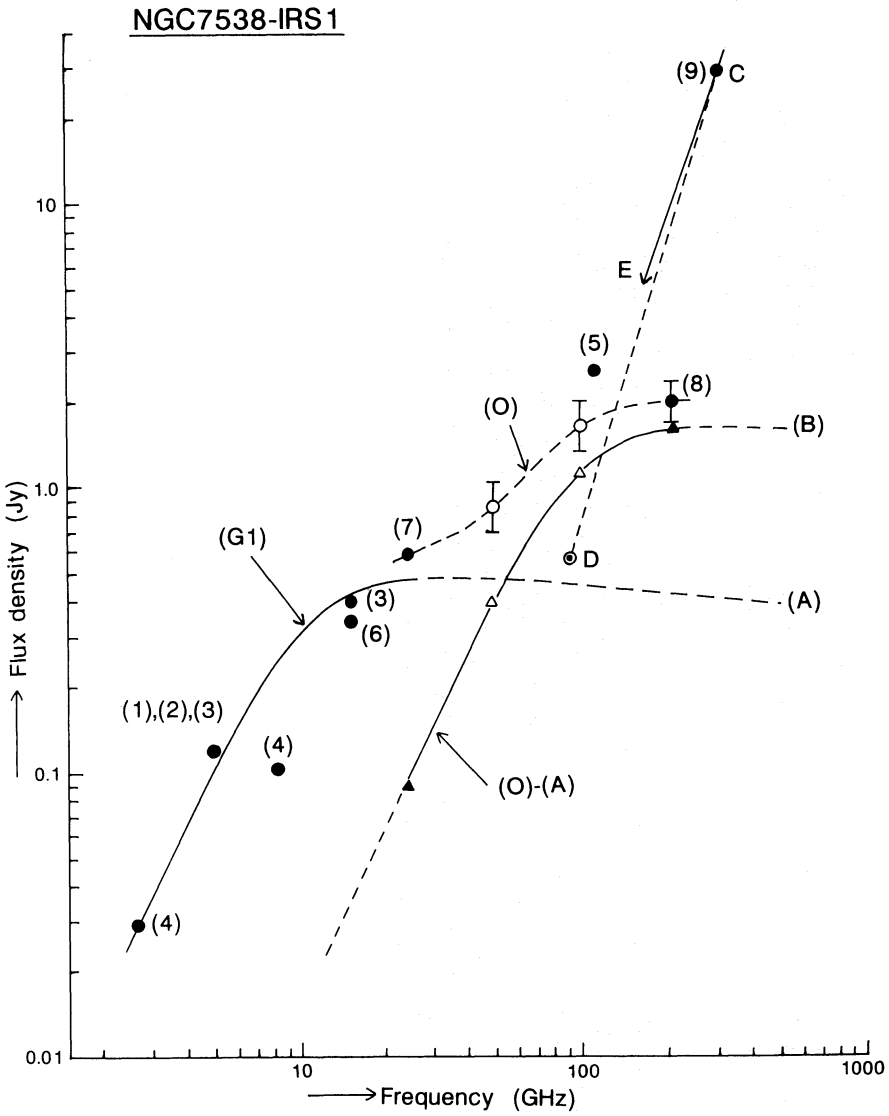

Fig. 6. Continuum spectra of the radio sources in NGC 7538 IRS1 called "G1" by Israel (1977). The present NMA results, (O) with open circles, were combined with those by other workers as (1): Martin (1973), (2): Israel (1977), (3): Campbell (1984), (4): Wink et al. (1975), (5): Scoville et al. (1986), (6): Turner and Matthews (1984), (7): Henkel et al. (1984), (8): Woody et al. (1989), and (9): Werner et al. (1979). Spectrum (A) is for Campbell's ultra-compact H II region (Campbell 1984), and spectrum (B), marked by open and filled triangles, is for the new H II source derived as (O)−(A).

3.3. IRS2 and IRS3

In figure 7, the flux densities of NGC 7538-IRS2 obtained from the present NMA observation are plotted by open circles along curve (B), with filled circles along (B), (1), (2), (7), and (12), by other workers' results of the region "G2" of NGC 7538 (Israel 1977). According to the 1.4-GHz result (12) by Habing et al. (1972) the computed thermal spectrum of (B) in figure 7 can be fitted to observational data which has a turnover frequency at around 2 GHz. The NMA results give a nearly flat, and then quite optically thin, spectrum in the short mm-wave region. The source is hardly resolved by the present 49-GHz NMA observation, as shown in figure 4; the 98-GHz NMA observation, however, shows a clearly resolved and somewhat complex structure of the region. The intrinsic source sizes of the IRS2 at both frequencies are almost equal, as shown in table 2. The map of figure 5 can be compared with the 2″ resolution 5-GHz map by Martin (1973); the center of the bright area is nearly coincident to each other, showing that this region is optically thin

Table 3. Flux densities of divided radio sources in NGC 7538-IRS1. The total flux density of IRS1 was divided into 3 components: Comp. (A) of the VLA compact by Campbell (1984) and by Turner and Matthews (1984), Comp. (B) of the NMA compact, present work, and Comp. (C) of the diffuse dust by Werner et al. (1979). Data (7) and (8) are from Henkel el al. (1984) and Woody et al. (1989), respectively. 90-GHz data are the results obtained by the present 45-m dish observation; the H II flux densities of Comp. (A) and Comp. (B) at 90 GHz, however, are estimated from those of the spectra (A) and (B) in figure 6 at 90 GHz.

Frequency	24 GHz [7]	49 GHz	90 GHz	98 GHz	219.5 GHz [8]
Total	0.6 Jy	0.9±0.2 Jy	2.0±1.0 Jy	1.6±0.3 Jy	2.0±0.3 Jy
Comp. (A)	0.5 Jy	0.5 Jy	0.45 Jy	0.5 Jy	0.4 Jy
Comp. (B)	0.1 Jy	0.4 Jy	1.0 Jy	1.1 Jy	1.6 Jy
Comp. (C)	...	...	0.6 Jy	...	...

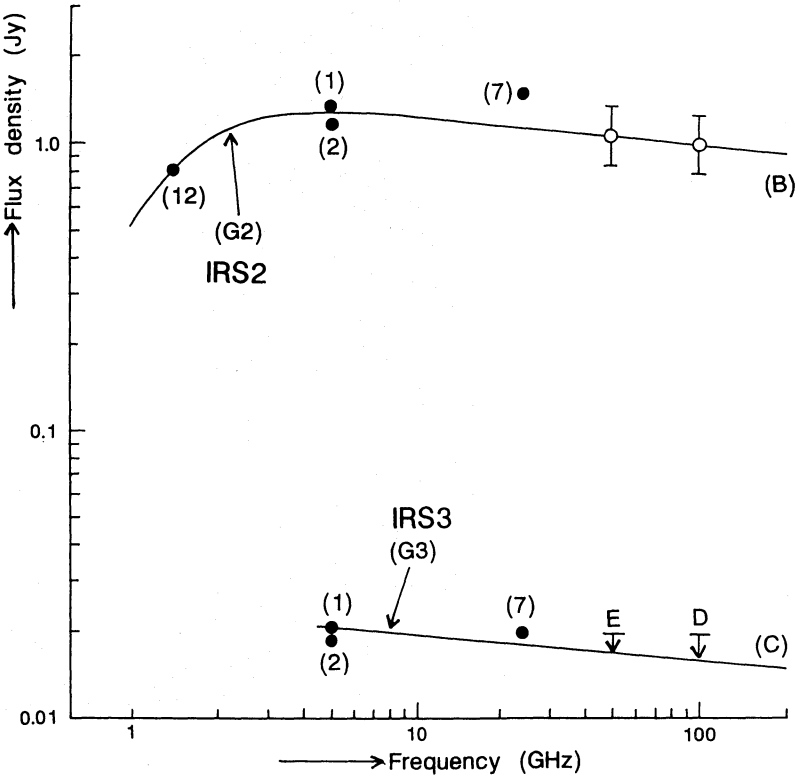

Fig. 7. Continuum spectra of the sources in NGC 7538 region. (B) is for IRS2 of the region, called "G2" by Israel (1977), where the present NMA results (open circles) were combined with cm-wave references, as noted in figure 6, (12): Habing et al. (1972), and Israel et al. (1973) being added. (C) is for IRS3 in the region, named as "G3" by Israel (1977), where the present NMA observation gives only upper limits of flux density D and E.

over a wide range of frequencies, although low brightness contours are missing in the 98-GHz NMA map. The center of the bright area also coincides with the position of IRS2 in the region (Wynn-Williams et al. 1974; Hackwell et al. 1982).

Straight line (C) in figure 7 is for a possible thermal H II spectrum of IRS3 in the region, noted as "G3" by Israel (1977), although the source was not detected by the present NMA observation at either 49 or at 98 GHz, as can be seen in figures 4 and 5. The E and D along line (C) give the upper limits of the flux densities ($\sim 2\sigma$) for an assumed point source of IRS3 at 49 and 98 GHz, respectively. The source seems to be optically quite thin down to 5 GHz; the linear size of the H II region (less than 1″.6) can be derived from the 5-GHz observation by Martin (1973), and by the VLA result by O. Kameya (private communication). New VLA 6-cm observations by Campbell and Persson (1988) have shown a resolved

Table 4. Physical parameters of H II sources in NGC 7538-IRS1, IRS2, and IRS3. The observational parameters for individual sources of the present work are summarized with reference to the VLA ultra-compact H II sources.

		Number of stars	n_e^2V/star (cm^{-3})	d(obs) (cm)	$\varepsilon_m(=n_e^2d)$ (cm^{-6} pc)	n_e (cm^{-3})	$t_i[=d(obs)/V_i]$ (yr)
	Campbell H II (A)	2 (B0)	0.85×10^{60}	2.3×10^{16} (0.″55×0.″55)	3.62×10^{8}	2.2×10^{5}	6.1×10^{2}
IRS1	NRO H II (1) (B)	1(O8.5)	7.2×10^{60}	6.7×10^{15} (0.″16×0.″16)	5.2×10^{10}	4.9×10^{6}	1.8×10^{2}
	NRO H II (2) (B)	4 (B0)	1.8×10^{60}	3.3×10^{15} (0.″08×0.″08)	5.2×10^{10}	6.9×10^{6}	9.0×10^{1}
IRS2		1(O9) 2(B0)	3.2×10^{60}	3.2×10^{17} (7″×7″)	6.2×10^{5}	7.7×10^{3}	8.5×10^{3}
IRS3		...	0.53×10^{59}	$\gtrsim2.2\times10^{16}$ (0.″53×0.″53)	3.6×10^{7}	$\lesssim7.1\times10^{4}$	5.8×10^{2}

map of IRS3 giving a linear size very close to 1″.0. No mm-wave excess emission was observed in the IRS3 region up to about 100 GHz.

4. Structure of the Radio Sources

4.1. NGC 7538-IRS1

We have assumed that the radio source in NGC 7538-IRS1 can be divided into at least two H II components, as shown in figure 6: one (A) of the VLA ultra-compact H II region by Campbell (1984), and the other (B) from the present work by the NMA and the 1.4-mm new result by Woody et al. (1989). The flux density ratio between components (A) and (B) in the completely optically thick range of frequencies is estimated as being about 30; this gives the ratio of the size of the emitting areas to be observed for the two components when the same electron temperature (T_e) is assumed for the two sources. A T_e of 8,000 K (as a working model) was adopted throughout this work. The source parameters which were derived under these assumptions are listed in table 4. The exciting parameter (Rubin 1968; Spitzer 1978), which is related to the surrounding H II volume emission measure (n_e^2V, where n_e is the electron density, and V is the volume of ionized region) will give central ZAMS O or B stars. The listed n_e^2V in table 4 were obtained from each observed flux density in the optically thin range of frequencies in figures 6 and 7 with a homogeneous n_e in V, and with the use of 2.8 kpc for the distance of the NGC 7538 region, as was used by Campbell (1984) and other workers. The source parameters for NRO H II [spectrum (B) in figure 6] were considered in two ways. NRO H II (1) in table 4 is for a single source, which gives spectral flux density, as shown by Comp. (B) in table 3; NRO H II (2) is for the case of 4 identical sources, each of which gives a quarter of the flux density of the Comp. (B), and is located separately to each other to give an intrinsic source size of $\sim 1''.2 \times 1''.2$, as noted in table 2. However, there is a strong possibility that a major part of Campbell's 14.965-GHz IRS1-N and IRS1-S sources (Campbell 1984) can be identified with the new NRO sources of (B) in table 4, even though the optical thickness in the mm-wave region of these ultra-compact H II sources is not well known. The d(obs) in the table is the source size determined from each observed thermal spectrum in figures 6 and 7 under an assumption that T_e is 8,000 K; for simplicity, $V = d^3$ was taken here with the d^2 area directed to the observer, instead of the spherical symmetry electron density distribution, as investigated by Turner and Matthews (1984). A T_e of 8,000 K is reasonably checked with the Campbell's (1984) spectrum (A) in figure 6, where the 5-GHz and optically thick flux density is well explained with the observed $\sim 1''.0 \times 0''.5$ size, and a T_e of 8,000 K. The emission measure [$\varepsilon_m(= n_e^2d)$] and then electron density (n_e) were derived from the thus-obtained n_e^2V and d. The $t_i[= d(obs)/V_i$, V_i being the isothermal sound speed in the H II region quoted by Davidson and Harwit (1967) as 12 km s^{-1}] is a measure of the time interval during which the source size could be doubled; the source could have a fourfold flux density in the optically thick range of frequency, as around 5 and 40 GHz for sources (A) and (B) in figure 6, respectively. Very short t_i were derived, raging from 10^2 to 10^3 yr, as shown in table 4. Then, an intensity monitoring observation of IRS1 at low frequencies, such as 5 to 40 GHz, as well as for the expansion of the source size, seems to be useful to investigate the evolution of extremely young H II sources, within a rather short time interval, such as 10 yr. In this case, a monitoring observation of the intensity ratio between IRS1 and IRS2 seems to be more effective to estimate the intensity increase of the IRS1 H II region.

H II sources, which are centrally condensed and ionized

with each central exciting star, as in the case of (A) and (B) in table 4, and are surrounded by the huge interstellar dust cloud (Wynn-Williams et al. 1974; Werner et al. 1979), can be well considered to be H II regions of the cocoon stars predicted by Davidson and Harwit (1967).

A mean straight line radio spectrum of IRS1 as ν^{-1}, for a single H II source, when it exists, from 2.695 to 219.5 GHz in figure 6 allows about a 50% observational error for each flux density. This might be attributed to a steady ionized gas flow of the stellar wind of central stars, which may introduce no substantial expanding features of an effective size of the ionized region.

4.2. NGC 7538-IRS2 and -IRS3

The same treatment as in IRS1 was made regarding sources IRS2 and IRS3; the physical results are listed in the lower part of table 4.

An H II extension of IRS2 ($\sim 7'' \times 7''$ corresponding to ~ 0.1 pc $\times$ 0.1 pc as in table 2) seems to be almost the same, or somewhat larger, than that of the 20 μm dust emission (Wynn-Williams et al. 1974); IRS2 would thus be in the end of its cocoon stage.

The volume emission measure ($n_e^2 V$) of IRS3 given in table 4 is too small to absorb the total flux of ionizing photons from an O or B star around its ZAMS. The situation of central star must therefore be before ZAMS, in which the total flux of ionizing photons would still be increasing. The source parameters of IRS3 given in table 4 were obtained under the assumption that there exists a turnover frequency at around 5 GHz in the spectrum of (C) in figure 7.

5. Conclusions

A continuum survey of the NGC 7538 region was made with the 45-m telescope at both 43 and 90 GHz. A strong mm-wave intensity excess was observed at the IRS1, 2, and 3 complex area in the region. This compact area was observed by NMA at both 49 and 98 GHz. Thermal H II spectra for IRS1, 2, and 3 were proposed, in the mm-wave region, and the IRS1 continuum was divided into two components: VLA ultra-compact H II and the other NRO H II. The H II sources in IRS1 can be well identified with those of the cocoon stars predicted by Davidson and Harwit (1967). We have suggested that the radio components in IRS1 may have a rather short evolution time, such as 100–1,000 yr. It is also suggested that the H II of IRS2 is extended, and is in the end of the cocoon stage, while IRS3 seems to be in a stage before the cocoon, because of its rather weak volume emission measure ($n_e^2 V$). A massive exciting star in IRS3 (if it exists) would, accordingly, be in a pre-main-sequence stage. A monitoring interferometer observation at around 49 GHz used to check the flux density ratio between IRS1 and IRS2 over 5 to 10 yr has been proposed; if a significant flux density increment of IRS1 is observed, we may deduce an expansion of the ionization front of the extremely compact and centrally condensed H II regions. The flux density ratio at 49 GHz, with a bandwidth of 80 MHz between IRS1 and IRS2, was estimated to be 0.8 ± 0.1 in 1988 December with a spatial resolution of $6''.0 \times 5''.5$ ($\Delta\alpha \times \Delta\delta$) by NMA.

The authors are grateful to the NRO engineers and operators for their collaboration and for the computer reduction. The authors also thank Dr. K.-I. Morita and Dr. N. Nakai for their valuable instructions during the observations. The authors used the NRO computer system with the program "CONDUCT" revised by Dr. T. Handa, and with the "AIPS" compiled by Dr. E. Fomalont et al. During this work, Prof. T. Nakano kindly encouraged the authors to study star evolution; this is heartily acknowledeged.

References

Akabane, K., Inoue, M., Kawabe, R., Ohashi, N., Kameya, O., Ishiguro, M., and Sofue, Y. 1991, *Proc. Astron. Soc. Australia*, **9**, 118.

Akabane, K., Sofue, Y., Hirabayashi, H., Inoue, M., Nakai, N., and Handa, T. 1985, *Publ. Astron. Soc. Japan*, **37**, 123.

Cambell, B. 1984, *Astrophys. J. Letters*, **282**, L27.

Cambell, B., and Persson, S. E. 1988, *Astron. J.*, **95**, 1185.

Davidson, K., and Harwit, M. 1967, *Astrophys. J.*, **148**, 443.

Gordon, M. A., Jewell, P. R., Kaftan-Kassim, M. A., and Salter, C. J. 1986, *Astrophys. J.*, **308**, 288.

Habing, H. J., Israel, F. P., and de Jong, T. 1972, *Astron. Astrophys.*, **17**, 329.

Hackwell, J. A., Grasdalen, G. L., and Gehrz, R. D. 1982, *Astrophys. J.*, **252**, 250.

Harris, S., and Scott, P. F. 1976, *Monthly Notices Roy. Astron. Soc.*, **175**, 371.

Henkel, C., Wilson, T. L., and Johnston, K. J. 1984, *Astrophys. J. Letters*, **282**, L93.

Israel, F. P. 1977, *Astron. Astrophys.*, **59**, 27.

Israel, F. P., Habing, H. J., and de Jong, T. 1973, *Astron. Astrophys.*, **27**, 143.

Kawabe, R., Inatani, J., Kasuga, T., Ishiguro, M., Yamamoto, M., Yamaji, K., and Watasawa, K. 1990, in *Proceedings of the 3rd Asia-Pacific Microwave Conference* (September 18–21, 1990, Tokyo), p. 217.

Lada, C. J., and Chaisson, E. J. 1973, *Astrophys. J.*, **183**, 479.

Martin, A. H. M. 1973, *Monthly Notices Roy. Astron. Soc.*, **163**, 141.

Mezger, P. G., and Henderson, A. P. 1967, *Astrophys. J.*, **147**, 471.

Panagia, N., and Felli, M. 1975, *Astron. Astrophys.*, **39**, 1.

Pratap, P., Batrla, W., and Snyder, L. E. 1989, *Astrophys. J.*, **341**, 832.

Rubin, R. H. 1968, *Astrophys. J.*, **154**, 391.

Schraml, J., and Mezger, P. G. 1969, *Astrophys. J.*, **156**, 269.
Scoville, N. Z., Sargent, A. I., Sanders, D. B., Claussen, M. J., Masson, C. R., Lo, K. Y., and Phillips, T. G. 1986, *Astophys. J.*, **303**, 416.
Sofue, Y., and Reich, W. 1979, *Astron. Astrophys. Suppl.*, **38**, 251.
Spitzer, L., Jr. 1978, *Physical Processes in the Interstellar Medium* (John Wiley and Sons, Inc., New York), p. 110.
Turner, B. E., and Matthews, H. E. 1984. *Astrophys. J.*, **277**, 164.
Werner, M. W., Becklin, E. E., Gatley, I., Matthews, K., Neugebauer, G., and Wynn-Williams, C. G. 1979, *Monthly Notices Roy. Astron. Soc.*, **188**, 463.
Wink, J. E., Altenhoff, W. J., and Webster, W. J., Jr. 1975, *Astron. Astrophys.*, **38**, 109.
Woody, D. P., Scott, S. L., Scoville, N. Z., Mundy, L. G., Sargent, A. I., Padin, S., Tinney, C. G., and Wilson, C. D. 1989, *Astrophys. J. Letters*, **337**, L41.
Wright, A. E., and Barlow, M. F. 1975, *Monthly Notices Roy. Astron. Soc.*, **170**, 41.
Wynn-Williams, C. G., Becklin, E. E., and Neugebauer, G. 1974, *Astrophys. J.*, **187**, 473.